

# Recrystallization Behavior of Single-crystal Hollow Blade Tenon

Liang Xiangfeng, Zhao Yutao, Jia Zhihong, Xu Weitai, Zhang Li

Jiangsu University, Zhenjiang 212013, China

**Abstract:** In order to better understand the effect of the temperature and load on recrystallization behavior of DD5 single-crystal hollow blade tenon, samples with different loads were heat treated at different solution temperatures in a furnace. Optical microscope and scanning electron microscope were used to study the microstructure of recrystallization and size distribution of  $\gamma'$  phase after solution treatment. Results show that there are no new grains found after solution treatment at 1230 °C/4 h, air cooling. However, the depth of load affected area increases with the bearing load and the size and depth of recrystallized cellular structure with newly-formed  $\gamma'$  phase particles increase with the load below the solution temperature. Besides, the recrystallized nuclei begin from the dendrite when the solution treatment is 1315 °C/4 h, air cooling. The dendrite arms are passivated and the boundary between dendrite arm and interdendritic space disappear and  $\gamma/\gamma'$  phase eutectic structure exists between dendrites in the recrystallization area. Moreover, the recrystallization area and the primary dendritic size gradually increase with the increase in load above the solution temperature.

**Key words:** single-crystal; recrystallization;  $\gamma'$  phase; dendrites; interdendritic; solution treatment

When the nickel-based single-crystal hollow blade used for aircraft engine is in the high-speed rotation state, in addition to the centrifugal load, vibration load and heat load, it also needs to withstand the corrosion and oxidation of environmental media, especially the blade tenon that bears the long-term interaction of gas and atmosphere media, so recrystallization occurs in the grain structure at high temperature, thus affecting the thermodynamic performance of the blade.<sup>[1-6]</sup> Therefore, it is very important to study the recrystallization behavior of single-crystal hollow blade tenon. Cox et al<sup>[7]</sup> studied the recrystallization behavior of CMSX-4 single-crystal alloy and found that the heat treatment temperature had a great effect on the single-crystal structure of plastic deformation. When the heat treatment temperature is above the solution temperature of  $\gamma'$  phase, the recrystal grains grow rapidly. On the contrary, the boundary growth of recrystal grains is inhibited. Zhang et al<sup>[8]</sup> studied the recrystallization behavior of DD3 single-crystal alloy and found that when the heat treatment temperature was above 1150 °C, the re-

crystal depth would increase rapidly with the increase in temperature. In addition, it is also found that the melting state of  $\gamma'$  phase is the key factor to determine the recrystallization behavior of nickel-based single-crystal alloy. Liu et al<sup>[9,10]</sup> studied the influencing factors of the recrystallization of nickel-based single-crystal alloy and found that with the increase in load intensity, the recrystallization area and depth would increase. Besides sub-crystal aggregation coarsening was the condition and growth mechanism of recrystallization nucleation of nickel-based single-crystal.

Despite of the numerous publications on recrystallization, reports associated with the recrystallization of single-crystal hollow blade tenon are rare. In the present work, to ensure the close alignment between the experimental results and industrial turbine material, DD5 nickel-based superalloy material with the high resistance against inelastic deformation and oxidation was used for preparing the single-crystal hollow turbine blade<sup>[11-15]</sup>. This paper discusses the recrystallization at low and high solution temperature.

Received date: November 25, 2017

Foundation item: Jiangsu Industrial Support Project (BE2014007-2, BE2014007-3, BE2014007-4); Jiangsu Development and Reform Commission ([2013]2027)

Corresponding author: Zhao Yutao, Ph. D., Professor, School of Material Science and Engineering, Jiangsu University, Zhenjiang 212013, P. R. China, E-mail: 18706102639@163.com

Copyright © 2018, Northwest Institute for Nonferrous Metal Research. Published by Elsevier BV. All rights reserved.

Optical microscope and scanning electron microscope were used to study the microstructure of recrystallization and size distribution of  $\gamma'$  phase after solution treatment, which could provide technical support for research and development of single-crystal hollow blade.

## 1 Experiment

The single-crystal sample was taken from the blade tenon for the recrystallization study and cuboids with the uniform size (3 mm×5 mm×7 mm) were obtained using wire-electrode cutting. The crystal growth direction has been marked, as shown in Fig.1. And then TH600 Brinell tester was used to apply different loads on the surface of 5 mm×7 mm in area, the hard alloy spherical indenter with a diameter of 5 mm was used in the hardness tester; the loading time for each sample was 15s, and the load test force were 500, 750, 1000 and 1500 kg. The cold deformation state of samples after loading different test forces are shown in Fig.2.

The heat-treatment regime was implemented according to the differential thermal analysis (DTA) curve of DD5 alloy, and the results are shown in Fig.3. The solidus and liquidus temperatures of DD5 are 1343.2 and 1386.1 °C, respectively, which means that the crystallization temperature range is 42.9 °C. The heat treatment window of DD5 alloy is in the interval where  $\gamma'$  is fully solid solution and eutectic structure is dissolved. However,  $\gamma$  is non-molten ranging from 1271.6 to 1343.2 °C. Consequently, the highest temperature in this heat treatment should be 1315 °C. This experiment included two groups of heat treatment process. The first group: 1230 °C/4 h, air cooling (AC), aiming to study the recrystallization form of blade tenon at the low solution temperature; the second group: 1315 °C/4 h/AC, aiming to study the recrystallization morphology when the heat treatment temperature is higher than the  $\gamma'$  phase remelting temperature. Then, the sample was cut in a direction perpendicular to the grain growth passing through the central position of indentation, as shown in Fig.1.

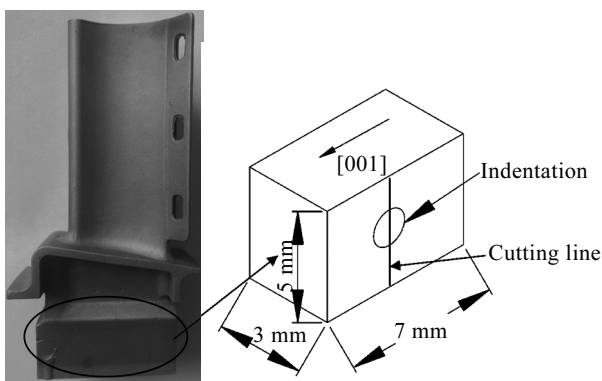


Fig.1 Diagrammatic sketch of recrystallization sample preparation

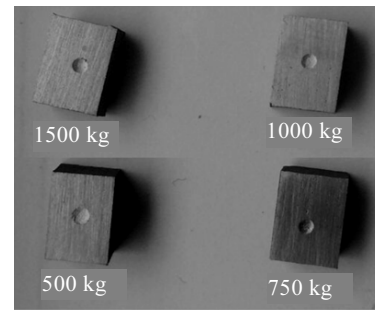


Fig.2 Cold deformation state of samples after loading test forces

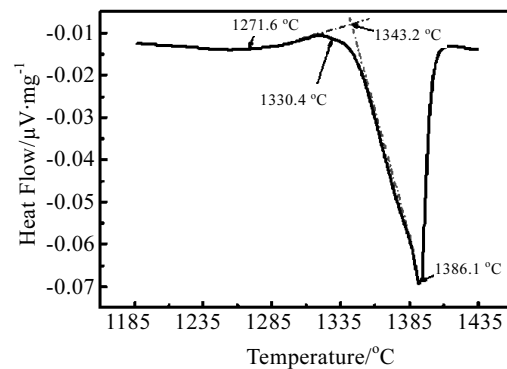


Fig.3 DTA curve of the DD5 single crystal alloy

## 2 Results and Discussion

### 2.1 Recrystallization at low solution temperature

Fig.4 shows the macrostructure of samples after solution treatment at 1230 °C/4 h/AC. It can be seen that there are no new grains found after the single-crystal samples received the solution treatment under different loads, indicating that no recrystallization occurs at 1230 °C. However, the white light area shows the morphology affected by the load and its structure is different from the original structure. The depth of white light area is increased with the increase in bearing load in the same solution treatment process.

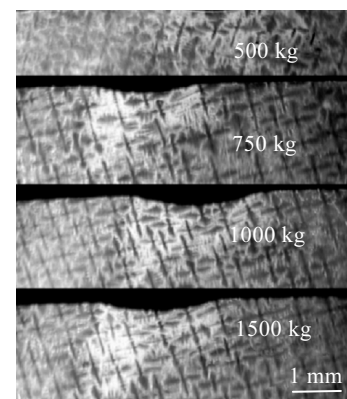


Fig.4 Macrostructures of samples after solution treatment at 1230 °C/4 h/AC under different loads

The dendrite morphology of affected area (Fig.5) and the unaffected area (Fig.5b) was observed by an Optical Microscope (OM). It can be known that the primary dendrite spacing between the two areas did not change significantly, but the interdendritic area in the affected area was increased, because the small  $\gamma'$  phases of interdendritic and dendrite arm in the affected area were dissolved, and the large  $\gamma'$  and  $\gamma/\gamma'$  eutectic structures were not dissolved, inhibiting the formation of recrystallization, so there were two scales of  $\gamma'$  phase between dendrites. In addition, a large number of  $\gamma'$  were dispersed around the undissolved eutectic structure between the dendrites in the affected area, but the above-mentioned phenomenon did not occur between the dendrites not affected by the load, as shown in Fig.5b and 5d. According to Energy Dispersive Spectroscopy (EDS) test (Fig.6), the element content of the large particles distributed dispersedly was almost the same as that of  $\gamma'$  phase, and the X-ray diffraction (XRD) analysis showed there was only one peak (Fig.7). Therefore, it can be concluded that the large particles distributed dispersedly are not the new phase of single-crystal sample produced in the heat treatment process, but the  $\gamma'$  phase coherent with  $\gamma$  phase re-precipitated during the cooling process after the heat treatment. The reason is that when cold deformation occurs in the single-crystal specimen bearing the load, the dendritic structure will slip, forming a large number of dislocations inside, which will be hindered and limited by the interdendritic  $\gamma/\gamma'$  eutectic structure in the process of movement, so that a large number of dislocations aggregate around the eutectic structure, forming sub-grain boundary. In the process of low temperature heat treatment, the solid

solubility of  $\gamma'$  phase forming elements in dendrite arm, such as Al and Ta, is low, but due to the accumulation of dislocations around the interdendritic  $\gamma/\gamma'$  eutectic structure and the increase of storage energy, the interdendritic dissolved  $\gamma'$  phase forming elements will spontaneously shift to the accumulation area of dislocations via the concentration and energy fluctuations, forming some small radicals rich in Ni, Al and Ta that is the sediment core of  $\gamma'$  phase formation. With the constant progress of atomic diffusion,  $\gamma'$  phase around the residual  $\gamma/\gamma'$  eutectic structure grows constantly, forming the coherent  $\gamma'$  phase as shown in Fig.5c.

Microstructure of samples after the heat treatment at 1230 °C/4 h/AC under different loads is shown in Fig.8. It can be seen that the recrystallization occurred in the form of cellular structure below the solution temperature, which was characterized by the fact that the new  $\gamma'$  phase particles near the recrystallization boundary were relatively large and the  $\gamma'$  phase particles at the centre of recrystallization were relatively small in equiaxed form. In addition, the  $\gamma$  phase matrix in the recrystallization structure still remained coherent with the newly-formed  $\gamma'$  phase particles and the crystal orientation of them was consistent. But the difference in recrystallization structure caused by the different loads was that the size and depth of recrystallized cellular structure increased with the increase of the load. It was clear that the number of recrystallized cellular structure was the least when sample bore 500 kg and the cellular structure was obvious when the load was increased by 1500 kg. This is because when the heat treatment temperature is lower than the  $\gamma'$  phase remelting temperature, only part of  $\gamma'$  phase with low melting point will be dissolved, and the dissolved  $\gamma'$

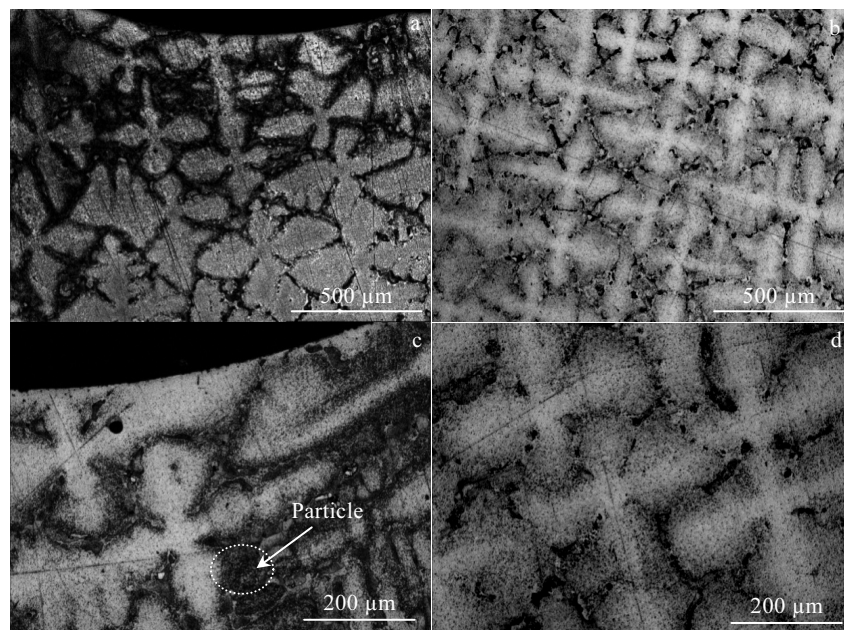


Fig.5 Dendrite morphologies of single-crystal samples after solution treatment at 1230 °C/4 h/AC: (a, c) affected area and (b, d) unaffected area

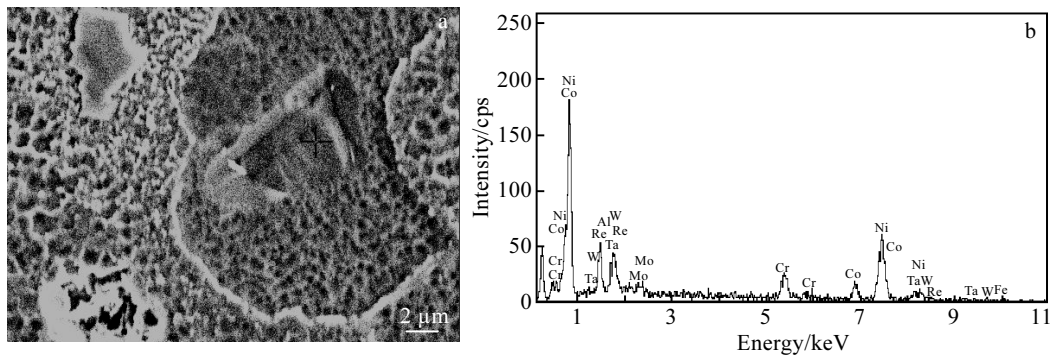


Fig.6 SEM image (a) and EDS spectrum (b) of the large particles distributed dispersedly in interdendritic of the affected area

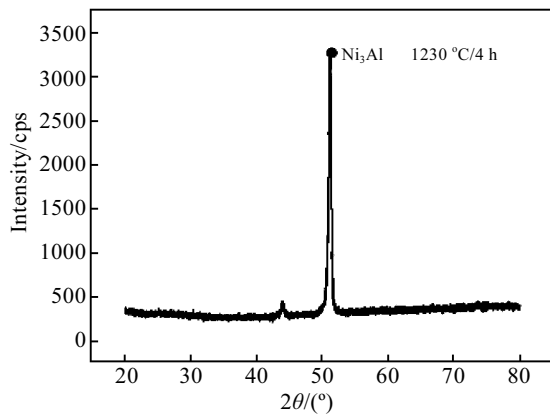


Fig.7 XRD pattern of the interdendritic area in the affected area

phase particles greatly improve the degree of supersaturation of solute atoms on recrystallization boundary. And they are precipitated by discontinuous precipitation during cooling process to reduce its supersaturation, thereby forming the recrystallized cellular structures. And this precipitation mode is related to the transmission speed of solute atoms on recrystallization boundary and the number of optional  $\gamma'$  phase nucleation sites. Generally, the faster the transmission speed is, the fewer the nucleation site is, the more easily the precipitation will occur. The storage energy of the deformed area increases with the load increasing. At the same time, the solution treatment process is the process of storage energy release, which is beneficial to the transfer of solute atoms in the recrystallization boundary, and the release of energy reduces the selectivity of  $\gamma'$  phase nucleation site. Therefore, at the same low solution temperature

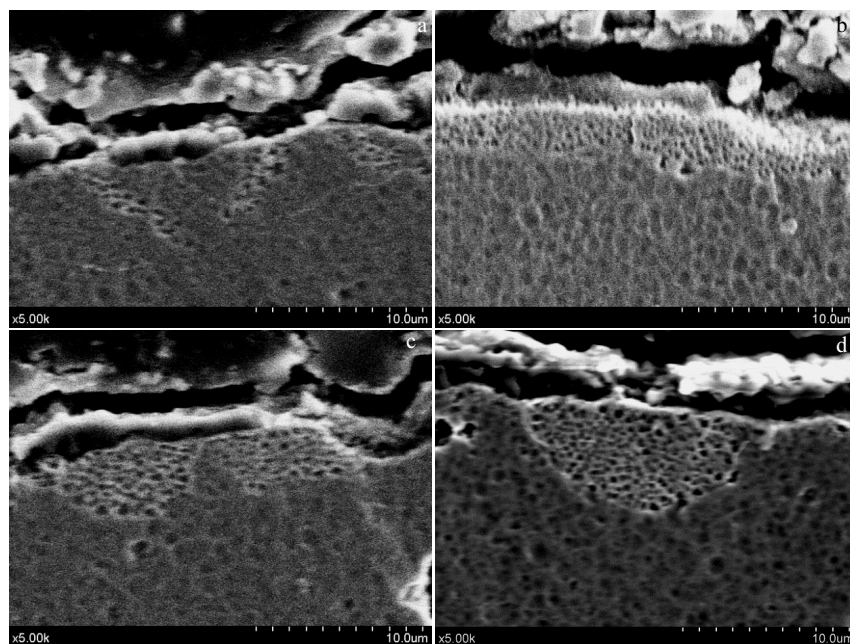


Fig.8 Microstructures of samples after the heat treatment at 1230 °C/4 h/AC under different loads: (a) 500 kg, (b) 750 kg, (c) 1000 kg, and (d) 1500 kg

the size and depth of recrystallized cell structure will increase with the load increasing.

## 2.2 Recrystallization at high solution temperature

Macro morphology of samples after the solution treatment at 1315 °C/4 h/AC is shown in Fig.9. It can be seen that the white light area was the recrystallization area, and the recrystallization nuclei were formed at the maximum distortion caused by plastic deformation. The recrystallization area and the primary dendritic size gradually increased with the increase of load, as shown in Fig.9 and Fig.10. When the load was 500 kg, the recrystallization depth was 0.9 mm, and when the load was 1500 kg, the recrystallization depth reached up to 2 mm. In addition, the brightness of dendrites in the recrystallization area was the highest, indicating that the recrystallized nuclei begin from the dendrite. Due to the recovery phase, the plastic deformation transforms the  $\gamma$  phase matrix of dendrite arm into sub-grain via polygonal transformation, some of which will gradually grow up, and develop into recrystallized nuclei. And the dislocations on the adjacent sub-grain boundaries, through the climbing and slipping, transfer to the surrounding sub-grain boundaries, leading to the disappearance of the original sub-grain boundary and then the orientations of two or more small-angle sub-grains become the same through the atomic diffusion and displacement adjustment, merging into a large sub-grain, namely the large-angle grain boundary. Sub-grain boundary nuclei can grow up and become recrystallized nuclei relying on the consumption of surrounding high-energy areas, so with the load increasing, the deformation quantity of load area will increase, thus increasing the storage energy in this area, forming more high-energy areas and promoting the formation of recrystallized nuclei.

The microstructure of recrystallization after solution treatment at 1315 °C/4 h/AC is shown in Fig.11. It can be seen that the dendrite arms in the affected area was passivated and the boundary between dendrite arm and interdendritic space disappeared,  $\gamma/\gamma'$  phase eutectic structure existed between dendrites, so it can be concluded that the  $\gamma'$  phase particles in dendrite arm area are dissolved first and recrystallization occurs. Due to the dissolution of  $\gamma'$  phase particles, the resistance to crystal boundary migration is reduced. The supersaturation of solute atoms is not high at the crystal boundary, combined with the higher solution temperature, the diffusion ability of crystal boundary is increased and the solute elements are precipitated at the end of recrystallized boundary. In the process of precipitation, the residual liquid phase between the newly-formed grains will reach the eutectic point, thus forming new  $\gamma/\gamma'$  eutectic structures. During the cooling process, the recrystallized structure exists in the form of intact grains and the  $\gamma'$  phase re-precipitated from crystal is dispersed in the  $\gamma$  matrix in small cubes, as shown in Fig.11b. In addition, it can be seen

from the recrystallization mode of dendrite arm in Fig.11a the plum blossom-like dendrite arms gradually fill the interdendritic space and the interface between the crystals is flat, which is because at the high solution temperature, the atoms have a large enough diffusion capacity. The atoms diffuse from the concave side to the convex side of crystal boundary, and crystal boundary moves towards the center of curvature. As a result, the crystals on the convex side grow constantly, and those on the concave side shrink and disappear until the crystal boundary becomes flat and the driving force of interface movement is zero, achieving a relatively stable state. The diagram of the crystal boundary movement is shown in Fig.12. Therefore, on the whole, the driving

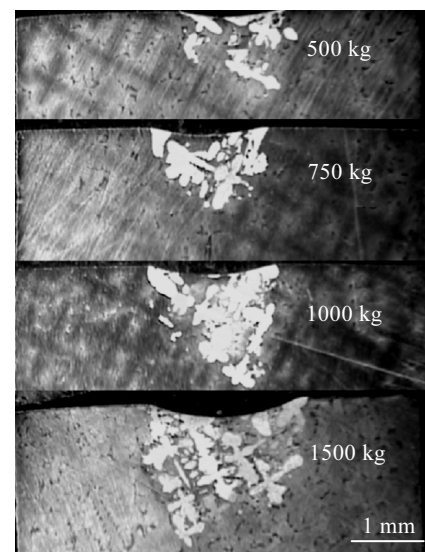


Fig.9 Macro morphologies of sample after solution treatment at 1315 °C/4 h/AC under different loads

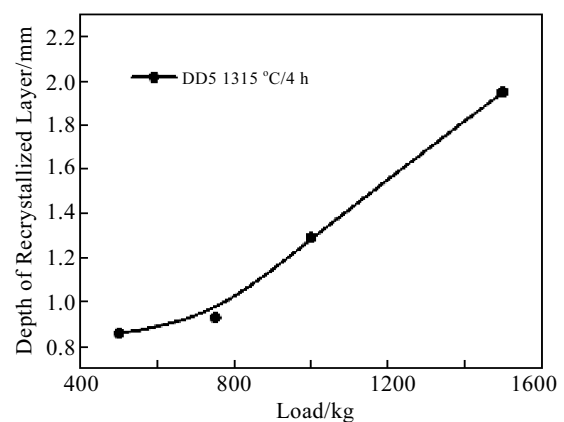


Fig.10 Relationship between the load and the recrystallization depth of DD5 alloy under the heat treatment of 1315 °C /4 h

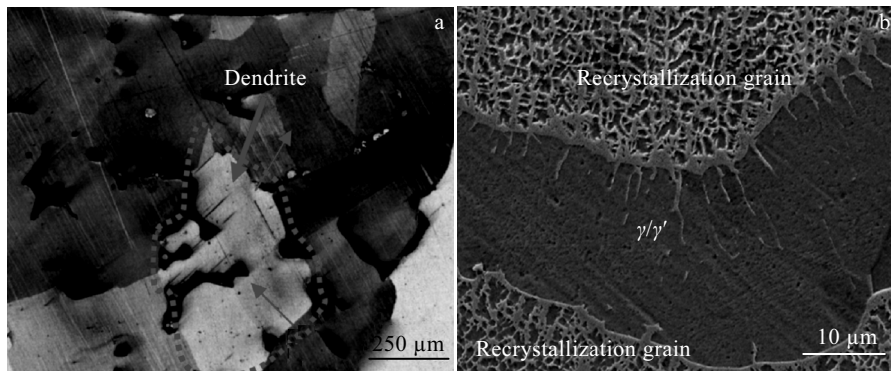


Fig.11 Microstructures of recrystallization: (a) dendrite and (b)  $\gamma'$  phase

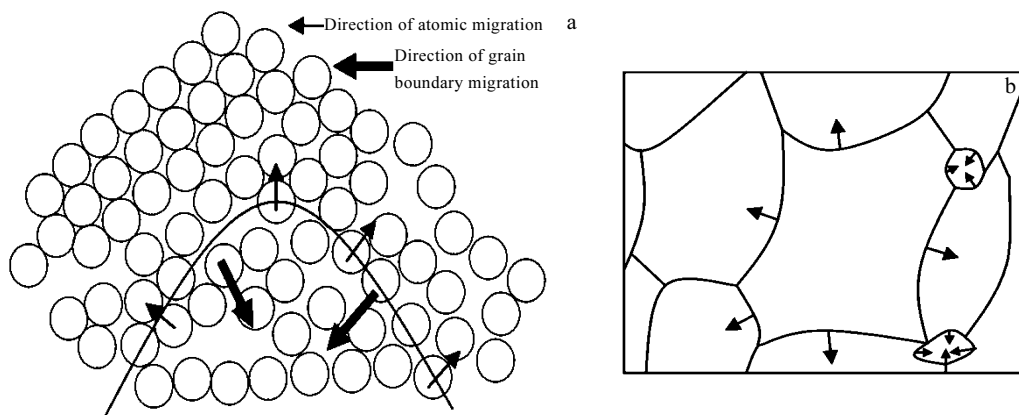


Fig.12 Schematic diagram of grain growth of recrystallization: (a) direction of atomic migration and (b) direction of grain boundary migration

force of crystal growth is the interfacial energy difference before and after the crystal growth. As the original dendrite arm shows the cross-shaped plum blossom-like structure, there are more crystal interfaces and higher interfacial energy, and the crystal growth into coarse crystal is the spontaneous process reducing the free energy of alloy. Therefore, at the crystal growth stage, the driving force of crystal boundary movement is proportional to its interfacial energy, but inversely proportional to the radius of curvature of crystal boundary. The greater the interfacial energy of crystal boundary is, the smaller the radius of curvature is, the greater the driving force of interface movement will be.

### 3 Conclusions

1) There are no new grains found after solution treatment at 1230 °C/4 h/AC. However, the depth of affected area is increased with the increase of bearing load and the size and depth of recrystallized cellular structure with newly-formed  $\gamma'$  phase particles increase with the load increasing below the solution temperature.

2) The recrystallized nuclei begin from the dendrite and form at the maximum distortion caused by plastic deformation when the solution treatment is 1315 °C/4 h/AC. The recrystallization area and the primary dendritic size gradually increase with the increase of load. The dendrite arms is passivated and the boundary between dendrite arm and interdendritic space disappears and  $\gamma/\gamma'$  phase eutectic structure exists between dendrites in the recrystallization area.

### References

- 1 Yang Liang, Li Jiarong. *Rare Metal Materials and Engineering*[J], 2015, 44(6): 1363 (in Chinese)
- 2 Fang Y W, Li Y H, He W F et al. *Materials and Design*[J] 2013, 43: 170
- 3 Khan M A, Sundarajan S, Natarajan S et al. *Materials and Manufacturing Processes*[J], 2014, 29(7): 832
- 4 Huang M, Zhuo L C, Liu Z L et al. *Materials Science and Engineering A*[J], 2015, 640: 394
- 5 Liang X F, Zhao Y T. *Key Engineering Materials*[J], 2014 575-576: 394

- 6 Zhang S H. *Journal of Materials Science & Technology*[J], 2011, 27(2): 107
- 7 Cox D C, Roebuck B, Rae C M F et al. *Materials Science and Technology*[J], 2003, 19(4): 440
- 8 Zhang Bing, Tao Chunhu, Lu X et al. *Journal of Iron and Steel Research International*[J], 2009, 16(6): 75
- 9 Liu Lirong, Zu Guoqing, Huang Jingsheng et al. *Transactions of Materials and Heat Treatment*[J], 2013, 34(3): 55 (in Chinese)
- 10 Liu Lirong, Zu Guoqing, Jin Tao et al. *Transactions of Materials and Heat Treatment*[J], 2013, 34(6): 38 (in Chinese)
- 11 Liang X F, Zhao Y T, Jia Z H et al. *International Journal of Minerals Metallurgy and Materials*[J], 2016, 23: 683
- 12 Zhang S M, Yu J G, Huang Z Y et al. *Rare Metal Materials and Engineering*[J], 2016, 45(5): 1147
- 13 Tian S G, Wu J, Shu D L et al. *Materials Science and Engineering A*[J], 2014, 616: 260
- 14 Liang X F, Zhao Y T, Ma D X. *Materials and Manufacturing Processes*[J], 2017, 32(16): 1887
- 15 Wu D, Tian L X, Ma C L. *Rare Metal Materials and Engineering*[J], 2015, 44(6): 1345

## 单晶空心叶片榫头再结晶行为研究

梁向锋, 赵玉涛, 贾志宏, 徐维台, 张 力  
(江苏大学, 江苏 镇江 212013)

**摘 要:** 为了更好的研究温度和载荷对镍基单晶空心叶片榫头位置的再结晶行为的影响, 首先对单晶试样施加不同载荷, 然后在不同的温度下进行固溶处理, 采用光学显微镜和扫描电子显微镜对处理后的试样进行组织分析。结果表明: 不同载荷下的 DD5 单晶试样经 1230 °C 保温 4 h 空冷后, 随着载荷增加, 受载荷影响区域深度增加, 该区域枝晶间空间增大, 未溶解的共晶组织周围弥散分布大量与  $\gamma$  相共格的  $\gamma'$  相颗粒,  $\gamma'$  相粒子以胞状形式重新析出, 尺寸和深度随载荷的增大而增加; 经 1315 °C 保温 4 h 空冷后发生再结晶现象, 随着载荷增加再结晶区域增大, 受载荷影响区域的枝晶干发生钝化, 枝晶干与枝晶间界限消失, 再结晶晶粒间存在  $\gamma/\gamma'$  共晶组织。

**关键词:** 单晶; 再结晶;  $\gamma'$  相; 枝晶干; 枝晶间; 固溶处理

---

作者简介: 梁向锋, 男, 1987 年生, 博士, 讲师, 江苏大学材料科学与工程学院, 江苏 镇江 212013, E-mail: lxf@ujs.edu.cn